Far-infrared absorption and ionic conductivity of Na, Ag, Rb, and K β-alumina

S. J. Allen, Jr., A. S. Cooper, F. DeRosa, J. P. Remeika, and S. K. Ulasi
Bell Laboratories, Murray Hill, New Jersey 07974
(Received 29 July 1977)

The far-infrared conductivity of Na, Ag, Rb, and K β-alumina is measured from 10 to 200 cm^{-1}. A broad band of absorption is observed whose detailed structure depends on growth conditions. The frequencies observed agree quantitatively with model calculations by Wang, Gaffari, and Choi (WGC) for the vibrations of the mobile ions. The ionic conductivity of Na, Ag, Rb, and K β-alumina obtained from a melt, a Bi_2O_3 flux, and a Co-doped Bi_2O_3 flux is also measured. Invariably the melt-grown material which has the lowest mobile-ion content has the higher conductivity, the pure flux-grown material the lowest, while the Co-doped material lies between the two. This result points to the crucial but subtle role played by the concentration of mobile ions, compensating defect, and the interaction between the two. Despite the variation of the observed conductivities with growth conditions, convincing correlations can be made between the vibrational properties, the model calculation of WGC, and the observed conductivities, that suggest that the basic jump mechanism is the interstitialcy and it is quantitatively described by the WGC model. It is suggested that the observed variation in conductivity are due to the inhibition of this mechanism by short-range order among the mobile ions and compensating defects.

I. INTRODUCTION

Solid electrolytes are an interesting class of compounds that exhibit anomalously high ionic conduction at temperatures well below their melting points. This property, when combined with mechanical strength and chemical stability, has stimulated the invention of novel electrochemical systems.[1-4] High-energy-density battery systems based on the Na-S couple made possible by the Na β-alumina solid electrolyte are a case in point.[5-7] Although the technology for producing such battery systems is quite advanced, our understanding of the microscopic interactions that permit high values of conductivity in solid electrolytes is at best somewhat primitive. Principles such as open, three-dimensional channels, with more available sites than mobile ions may provide good guides for synthesizing new materials, but do not provide us with good quantitative understanding of the interactions that ultimately inhibit or enhance ionic conduction in these systems. Although the advanced development of these technologies proceeds apace irrespective of detailed understanding of some of the more fundamental questions concerning fast-ion transport in solid electrolytes, the long-term development of these sophisticated electrochemical systems may be aided by improving our understanding of the properties of these materials at a more fundamental, atomic level.

There are two basic questions that may be addressed in studying solid electrolytes. (i) What stabilizes the open structures that permit fast-ion transport, or what causes the transition from a normal ionic solid to the electrolyte phase as is seen in the classic AgI? (ii) Given that we have an open structure supporting fast-ion transport, how do the various microscopic interactions influence the ion conduction, or what is the role of mobile-ion–mobile-ion interaction, and mobile-ion–host interaction?

In the case of the β-aluminas, the first question is probably answered with difficulty. β-alumina is a ternary compound with a somewhat extended crystal structure,[8-12] shown in Figs. 1 and 2, and to obtain a good understanding from a theoretical view of its particular morphology is beyond present discussion. However, Sato and Hirotsu[13] have made some interesting suggestions with regard to stacking of spinel and diffusing layers that are relevant to this question. A related but more restrictive question may be asked in the context of β-alumina. What causes the deviation from stoichiometry and how is it compensated? It is believed that the high ionic conduction is related to the presence of excess mobile cations due to some other immobile compensating defects. Two mechanisms have been put forward for the compensation: Al^{3+} vacancies in the spinel block[14] and extra O^{-2} as an interstitial in the mirror plane[15,16] (Fig. 2). X-ray crystallographic data have confirmed that O^{-2} interstitials do reside in the mirror or conduction plane and are bound there by Al^{3+} Frankel defects.[15,16] The possibility of Al^{3+} vacancies is somewhat uncertain but has not been ruled out. Invariably, Na β-alumina is found with the excess Na but crystal chemical arguments as to why it should do so are hard to come by. Reidinger[17] has argued that such behavior is reasonable since the stoichiometric crystal would have excess plus charge buildup in the layers near

the conduction plane and the deviation from stoichiometry relieves this imbalance.

Diffuse x-ray scattering[18-20] has shed considerable light on the organization of the diffusing species and the interstitial oxygen. The correlation length for short-range order has been shown to depend on growth conditions and diffusing species.[18] No detailed models exist that relate the short-range order to diffusion but the trend for the best conductors to be more highly disordered is apparent and reasonable.

Most of the microscopic experiments or probes of β-alumina to date have been more concerned with the second question: Given that β-alumina is a solid electrolyte with a large deviation from stoichiometry, what are the microscopic interactions that control diffusion in this system? These probes include measurement of the correlation factor,[14,21] inelastic neutron scattering,[22,23] nuclear magnetic resonance (NMR),[24-27] specific heat,[28] thermal conduction,[29] Raman scattering,[30,31] microwave absorption,[32-34] internal friction,[35] and infrared absorption.[33-38]

Of the above experiments, the correlation factor[14,21] and NMR[24-27] directly relate to the ionic conductivity or diffusion coefficient. The correlation factor or Haven's ratio was first obtained by Whittingham and Huggins[14,21] for Na and Ag β-alumina and found to be ~0.6 for both. A value of 0.6 is expected for an interstitialcy mechanism if the interstitial is located on the anti-Beevers-Ross site. Since Na does not occupy the anti-Beevers-Ross site, the results are somewhat ambiguous. The temperature dependence of the nuclear spin-lattice relaxation time directly samples the hopping motion of the relaxing nucleus. Walstedt *et al.*[27] have been able to measure distributions of activation energies for β-alumina obtained from different sources. Striking differences are observed for the melt- and flux-grown material which can be related to differences in conductivity. At the same time, remarkably low values of attempt frequency are obtained, which is a major shortcoming in our understanding of the diffusion process. These low-attempt frequencies are confirmed by experiments on relaxation absorption.[35]

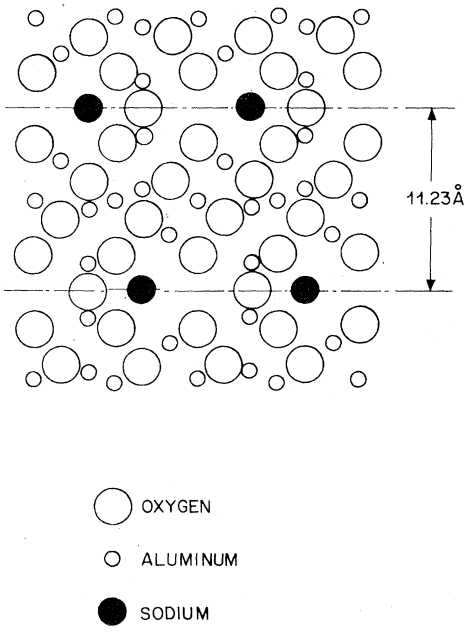

FIG. 1. Section through Na β-alumina perpendicular to the [110] direction. Two diffusion planes are indicated.

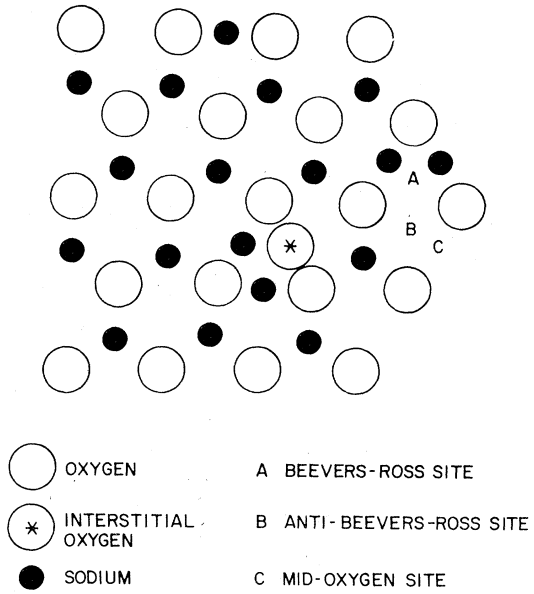

FIG. 2. Mirror or diffusion plane in Na β-alumina. An interstitial oxygen and extra sodium are indicated.

The remaining experiments probe in some sense the small-amplitude vibrations of the ions. The subject of this paper concerns one such probe, the infrared absorption of conductivity of Na, Ag, Rb, and K β-alumina. Portions of this work have been published elsewhere.[37,38] The work is intimately connected with the specific heat[28] and inelastic neutron scattering reported by McWhan *et al.*,[22,23] the Raman scattering of Hao, Chase, and Mahan,[30,31] and previous reports of infrared and microwave absorption on Na and Ag β-alumina by Armstrong *et al.*,[36] Barker *et al.*,[33,34] and Strom *et al.*[32] These relations will be explored below.

The diffusion process is a large-amplitude

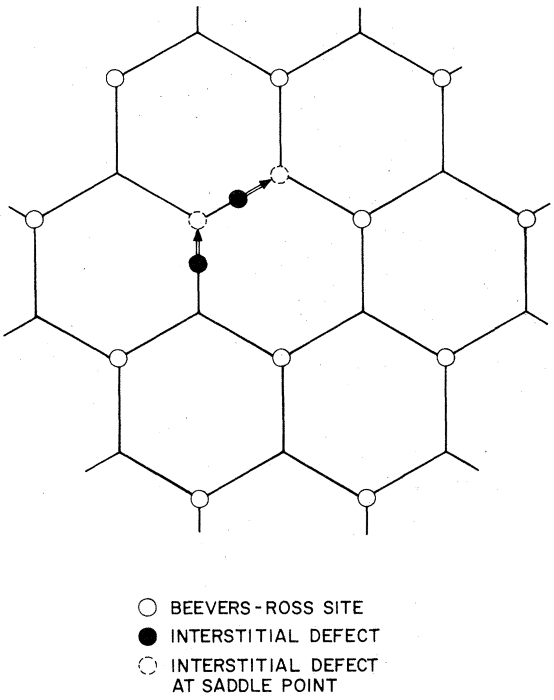

FIG. 3. Hexagonal net of Beevers-Ross, anti–Beevers-Ross sites. An interstitial defect caused by an excess mobile ion moves as indicated to the saddle point to execute the basic jump in the interstitialcy mechanism (Refs. 14, 21, and 40).

fluctuation of the ion position and hence can be only connected to the small-amplitude or harmonic motion by some theoretical model. In an earlier publication, we relied on the model of Sato and Kikuchi.[39] In the present work, we find it more profitable to use the theoretical calculations of Wang, Gaffari, and Choi,[40] (WGC) to carry us from the observed vibrational frequencies of the diffusing species to the dc conductivity. In Fig. 3, we show the interstitial pair which forms the key element in the interstitialcy jump and the model calculation of WGC.

The infrared results are interesting only to the extent that they can be related to the transport properties. Yet is should be clear that the conduction in the β-aluminas is a defect-related property and as such should depend on growth conditions and chemical content. To facilitate a comparison between the far-infrared and dc transport, we have also systematically studied how the temperature-dependent conductivity depends on growth conditions and on chemical composition. These results are also presented and discussed.

We find that the interaction potential proposed by WGC predicts the vibrational properties seen in the infrared, low-temperature specific heat, and Raman scattering. The interaction potentials applied to an interstitialcy mechanism give semiquantitative agreement with observed prefactors and activation energies. We conclude that the basic motion is interstitialcy and the interaction potentials are properly parameterized by these model potentials. At the same time important differences between melt-, flux-, and Co-doped flux-grown material are observed that point to the crucial role played by compensation and short-range order.

II. SAMPLE CHARACTERIZATION

The Na β-alumina used in this investigation came from two sources: Melt-grown material purchased from Union Carbide characterized by a high growth temperature $\approx 2000\,^{\circ}\mathrm{C}$ and material grown from a Bi_2O_3 flux at temperatures $\leq 1300\,^{\circ}\mathrm{C}$. Two types of flux-grown material were studied; a pure Na β-alumina and a Co-doped Na β-alumina and their suitably cation exchanged isomorphs. X-ray powder patterns did not detect any β''-alumina in the samples studied. Spectroscopic analysis revealed no Bi (<10 ppm) in flux-grown crystals with no visible flux inclusions.

The weight change upon exchange gave the following excess mobile-ion content:

melt β-alumina $\approx 0.16 \pm 0.03$,

flux β-alumina $\approx 0.38 \pm 0.03$,

flux Co-doped β-alumina $\approx 0.38 \pm 0.03$.

It is also important to note that the melt-grown material has roughly $\frac{1}{2}$ the extra mobile cation as does either of the flux-grown materials.

The Co-doped material deserves special attention. The Co to Al ratio in the melt is 0.0101. Chemical analysis indicates a distribution coefficient for Co of 1.06.[41] Then for the Co-doped sample, there is enough Co^{2+} to compensate $\frac{1}{3}$ of the excess mobile cation. In the Co-doped sample $\frac{1}{3}$ of the compensation is valence deficiency in the spinel block and $\frac{2}{3}$ O^{-2} interstitial in the diffusion plane.

The material used in this study was the same as that used by McWhan *et al.* for a study by diffuse x-ray scattering (see the following paper).

III. FAR-INFRARED CONDUCTIVITY

A. Results

The far-infrared conductivity was determined from ~10 to 200 cm^{-1} by measuring the transmission through thin (≈ 50-μm) sections mounted on crystal quartz wedges. Only the pure melt- and

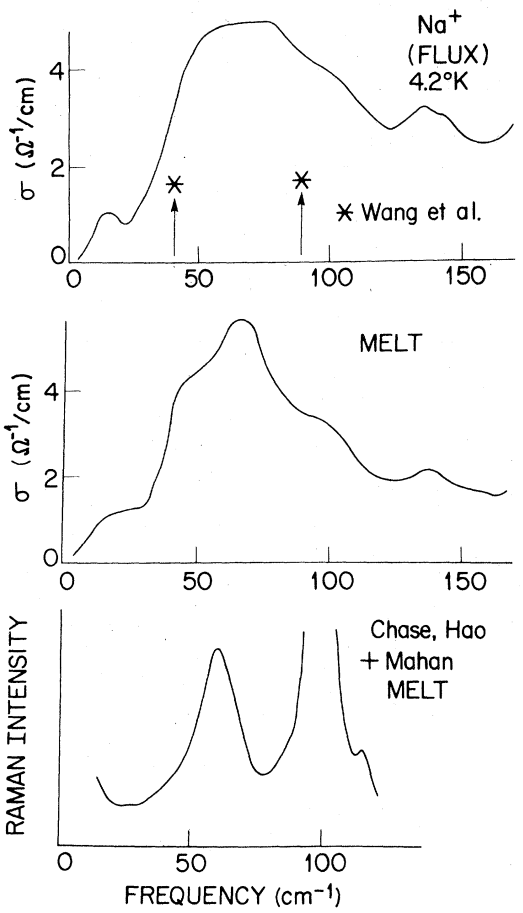

FIG. 4. Conductivity of Na β-alumina in the basal plane, room temperature except where indicated. Raman scattering from Refs. 30 and 31.

flux-grown samples were studied. The imaginary part k of the complex refractive index $n+ik$ is given by

$$k = -\frac{1}{4\pi t\nu} \ln T , \tag{1}$$

where T is the transmission, t is the thickness of the sample in cm, and ν is the frequency in cm^{-1}. For weak absorption, the real conductivity is directly found from

$$\sigma(\nu) = 2\pi c\nu\epsilon_2(\nu) , \tag{2}$$

where c is the velocity of light and ϵ_2 is the imaginary part of the dielectric constant given by

$$\epsilon_2(\nu) = 2nk , \tag{3}$$

where n is the real refractive index. n may be taken as 2.8 for β-alumina in the frequency range of interest.

For Na and Ag, the absorption is strong and considerable dispersion in n is observed. In this

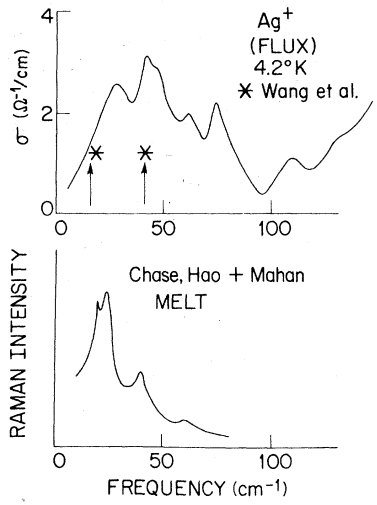

FIG. 5. Conductivity of Ag β-alumina at 4.2 °K. Raman scattering from Refs. 30 and 31.

case, n is found by Kramers-Kronig analysis of the directly measured $k(\nu)$ by

$$n(\nu) = n_\infty + \frac{2}{\pi}\int_0^\infty \left[\frac{k(\nu')\nu' - k(\nu)\nu}{\nu'^2 - \nu^2}\right] d\nu . \tag{4}$$

However, even in the case of Na and Ag where the index of refraction increases from 2.8 above the resonance to ~3.5 below, the corrections to the absorption line shape are modest and $\lesssim 20\%$.

It was found that prolonged exposure to room atmosphere produced irreversible increases in the background absorption in this frequency range. Consequently, the data reported here were taken only on samples that were either freshly exchanged

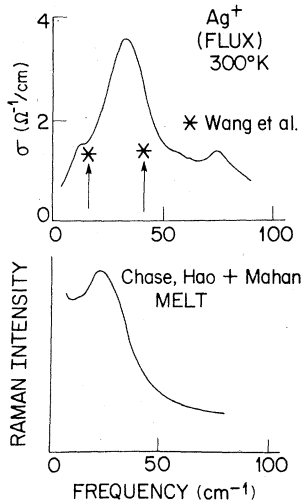

FIG. 6. Conductivity of Ag β-alumina, room temperature. Raman scattering from Refs. 30 and 31.

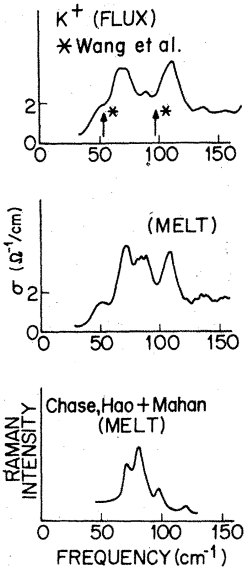

FIG. 7. Conductivity of K β-alumina, room temperature. Raman scattering from Refs. 30 and 31.

or stored when necessary in a vacuum desiccator.

The results are shown in Figs. 4–8. Only in the case of Ag is there a substantial temperature dependence of the spectra between 300° and 4.2°K. This was first observed by Chase *et al.*[31] There are striking differences not only between melt- and flux-grown material but also between the Raman scattering and infrared absorption. These will be discussed below.

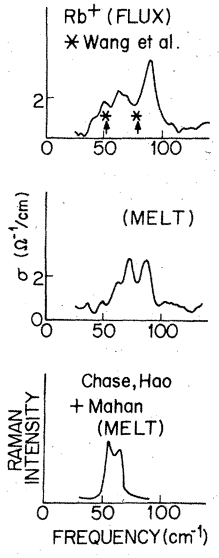

FIG. 8. Conductivity of Rb β-alumina, room temperature. Raman scattering from Refs. 30 and 31.

TABLE I. Effective charge from sum role, 300°K (estimated uncertainty ±30%).

	Na	Ag	K	Rb
Melt	1.7		1.4	1.6
Flux	1.6	1.9 (2.1 at 4.2°K)	1.5	1.5

In the absence of local-field corrections, the integrated absorption should be related to the number density of ions and their mass through the sum rule.

$$\int_0^\infty \sigma(\omega)\, d\omega = \frac{\pi}{2}\frac{N(Ze)^2}{M}\ , \tag{5}$$

where N is the number density, M is the ion mass, and Ze is the charge on the ion. We have evaluated the sum rule in (5) and expressed the result as an effective Z_{eff}. Background subtraction and the extended character of the spectra lend considerable uncertainty to the determination of Z_{eff}. We estimate uncertainties of the order of ±30%. The values of Z_{eff} are given in Table I. The values are constant within experimental error and imply that there is more than enough absorption strength to account for all of the mobile ions in β-alumina. We cannot exclude the possibility that only a fraction of mobile ions absorb in this frequency range but that their effective charge is even larger. This seems, however, unlikely. We have examined Li β-alumina but find no appreciable absorption in this range despite the fact that it should have approximately three times the integrated intensity of Na. $[M(\text{Na})/M(\text{Li}) \approx 3]$. No Raman scattering has been detected that can be ascribed to the Li.[30,31]

B. Discussion

The sensitivity of the spectra to cation substitution and scaling of the integrated absorption with the inverse mass leaves little doubt that the spectra are due to the mobile cation. The apparent complexity of the spectra is quite likely due to the disorder in the diffusion plane; some ions sit in the Beevers-Ross site, others in the mid-oxygen position either near a compensating defect or far from it.

WGC have calculated the vibrational frequency of the single ion sitting in the Beevers-Ross site and the in phase motion of a pair sitting at mid-oxygen positions around a vacant Beevers-Ross site. These frequencies are indicated in Figs. 4–8. The low-frequency arrow in every case is the pair frequency. In two respects this comparison with experiment is not justified. In

some sense the frequencies calculated by WGC are zone-boundary excitations, excitations obtained by holding most of the ions fixed but allowing the ion in question to vibrate. The far-infrared response is a collective in-phase response of the entire system. However, Hsu[42] has calculated the vibrational spectrum as a function of wave vector $\vec{k}$ with WGC's potentials. In this more detailed calculation, the low-frequency features are still closely identified with the in-phase motion of the pairs and the higher-frequency features are either single-ion modes or out-of-phase motion of pairs. If the breadth of the spectra are related to differing configurations and environments, we may take the separation between the single ion and pair modes as a measure of the breadth produced by the WGC model. The success with which WGC predict the position and breadth of the absorption spectra for each of the cations indicates that the potentials of WGC are an accurate parameterization of the interaction between the mobile cation and the β-alumina host. We must, however, point out that the agreement obtained for Ag must be fortuitous. As WGC point out, the equilibrium position for Ag is not correctly predicted by their model; hence, the vibrational frequencies, although correct, are not based on realistic interaction potentials.

Recently Klein *et al.*[43] have also reported Raman and infrared absorption experiments on Na and K mixed β-alumina. They observe a quadratic dependence of the low-frequency structure on K content and ascribe it to the vibrations of a K interstitial pair as described by WGC.

It is interesting to note that the Raman scattering does not seem to reflect all of the structure seen in infrared absorption. Assuming that the above interpretation is correct, one is inclined to suggest that the Raman scattering is specific to the low-frequency vibrations of the interstitial pairs. This is not expected and cannot be justified on the basis of symmetry arguments.

The specific-heat experiments of McWhan *et al.*[28] relate directly to the infrared vibrations reported here. Indeed, the specific heat was fit using distributions of normal modes consistent with the far infrared. This has an important implication. The statistical weight assigned to the modes accounts for all the mobile cations. Then it is inappropriate for us to suggest that there are other modes at much lower or higher frequencies involving a significant number of mobile cations. Clearly there are low-frequency modes that do contribute to excess specific heat at low temperatures[32,33] but the effective number of ions that participate in these vibrations must be a small fraction of the total number of mobile cations.

We may conclude from the vibrational properties that the collection of mobile cations vibrate over a band of frequencies. These frequencies are determined largely by the local interaction of the mobile ion with the host lattice. The low-frequency portion of the band of excitations is probably related to the motion of the weakly bound interstitial pair.

IV. CONDUCTIVITY

A. Results

The ionic conductivity of all three types of β-alumina was measured with blocking electrodes by applying a fast voltage pulse and measuring the resulting current flow through a 50-Ω resistor (see Fig. 9). If the interfacial capacitance between the electrode and sample is sufficiently large, the conductivity of the sample may be determined by measuring the current flow near the leading edge of the pulse.

In practice, the rise time of the amplifier prevents one from measuring the current flow arbitrarily close to the leading edge. The criterion for a satisfactory contact is that the time constant for charging the interfacial capacitance C through the sample resistance R, $\tau_c = 1/RC$, be much longer than the rise time of amplifier, τ_r (in this case, $\tau_r \approx 0.1$ μsec). For the highly resistive samples, Rb and K, β-alumina, Engelhard platinum paste was sufficient, whereas for the Ag and Na samples Cr-Au evaporated contacts were necessary. Ultimately all measurements were performed with Cr-Au contacts. Typical charging time constants τ_c were $\gtrsim 20$ μsec.

The results are shown in Figs. 10–13. In Tables II and III, we collect the prefactors and activation energies for the four cations studied.

B. Discussion

There are a number of interesting and important correlations that can be made with regard to the

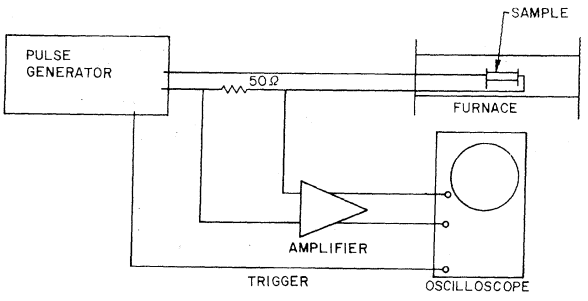

FIG. 9. Circuit used to measure ionic conductivity by pulse method.

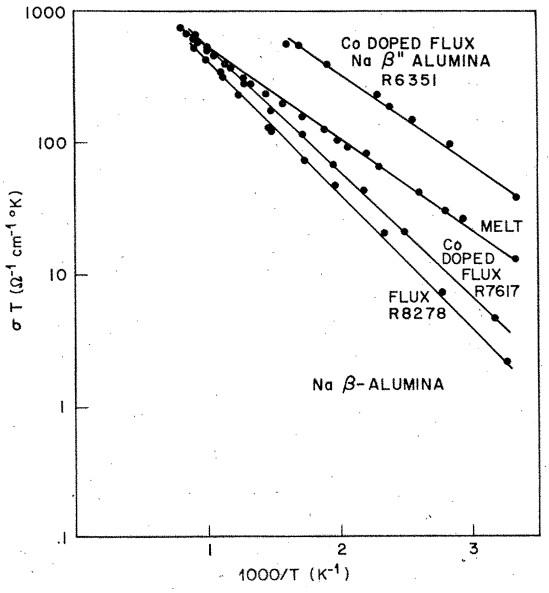

FIG. 10. Ionic conductivity vs temperature Na β-alumina. Au-Cr evaporated contacts. Increasing Co by tenfold in the flux gives Na β''-alumina and is shown for comparison.

TABLE II. Prefactors ($10^3\ \Omega^{-1}$/cm °K).

	Na	Ag	K	Rb
Melt	2.8±0.5	1.9±0.2	2.4±0.7	2.5±0.5
Flux, Co	5.2±0.5	2.5±0.5	3.0±0.5	4 ±1
Flux	4.8±0.5	7.8±1	7.5±1	5 ±1

data shown in Figs. 10–13. By weight exchange the melt-grown material has approximately $\frac{1}{2}$ the excess mobile cation of the flux-grown material, yet the conductivity is substantially larger in every case. Increasing the mobile-ion content does not necessarily increase the conductivity (see Kennedy and Sammells[44]). The prefactor does appear to increase as expected, but the activation energy also increases, giving lower conductivity in the temperature range of interest.

On the other hand, the two flux-grown samples also differ despite the fact that the mobile-ion content is the same. This is a clear indication that the type of compensation plays a crucial role in inhibiting the conductivity. The Co-doped sample has sufficient Co^{2+} to account for $\frac{1}{3}$ of the excess mobile cation. Removing the O^{2-} interstitial in the diffusing plane should improve the conductivity for two reasons. (i) The Co^{2+} in the

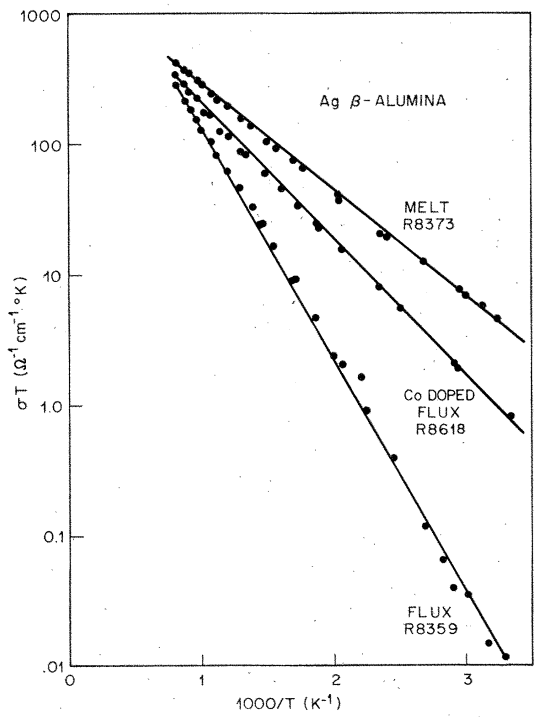

FIG. 11. Ionic conductivity vs temperature Ag β-alumina. Au-Cr evaporated contacts.

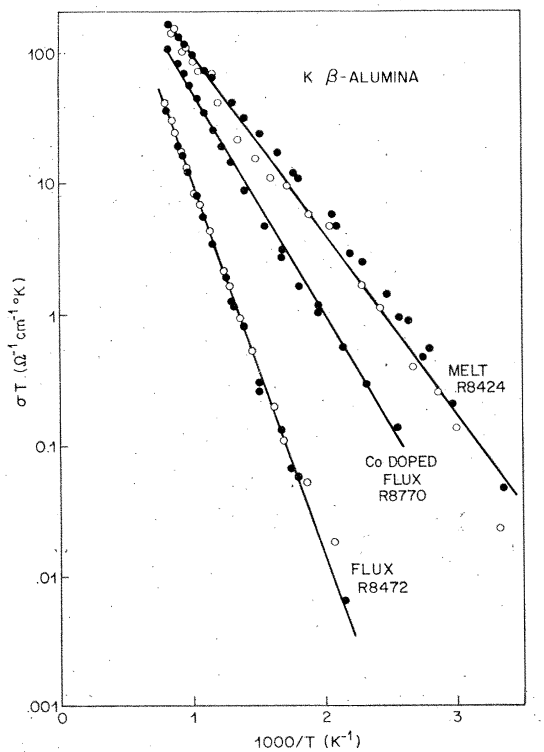

FIG. 12. Ionic conductivity vs temperature K β-alumina. ●—Au-Cr evaporated contacts, ○—platinum paste.

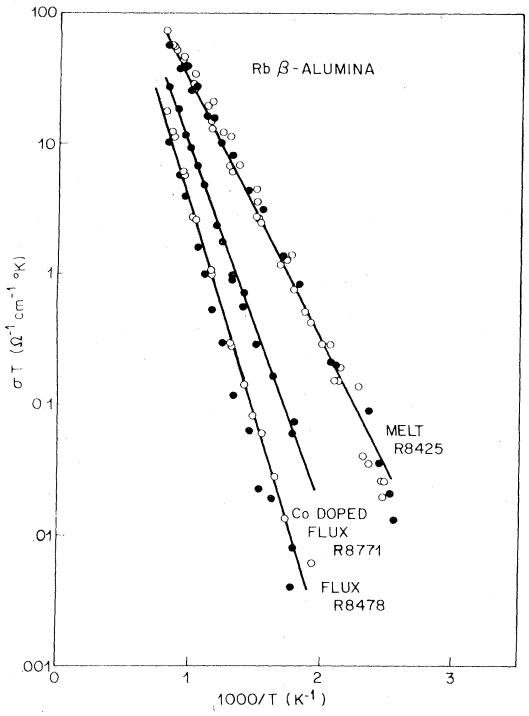

FIG. 13. Ionic conductivity vs temperature Rb β-alumina. ●—Au-Cr evaporated contacts, ○—platinum paste.

TABLE III. Activation energy (eV).

	Na	Ag	K	Rb
Melt	0.14±0.02	0.16±0.02	0.28±0.03	0.39±0.03
Flux, Co	0.19±0.02	0.21±0.02	0.34±0.02	0.54±0.03
Flux	0.20±0.02	0.35±0.03	0.56±0.02	0.65±0.04

spinel block does not impede flow in the diffusing plane. (ii) The Co^{2+} center is less charged and further away than the O^{2-} interstitial making it less attractive for binding the mobile ion to the compensating defect.

One remaining correlation should be drawn. X-ray diffuse scattering indicates that the flux-grown material, be it Co-doped or undoped, is more highly ordered than is the melt-grown material. The Co-doped material appears slightly less ordered than the undoped flux-grown material. Perhaps the crucial parameter is the degree of short-range order which depends on mobile-ion content and type of compensation. Clearly, this point of view deserves a more thorough examination.

We can also project these results on the theory of WGC. This we do in Figs. 14–16, where we compare the observed activation energy versus that predicted by the low-frequency edge of the

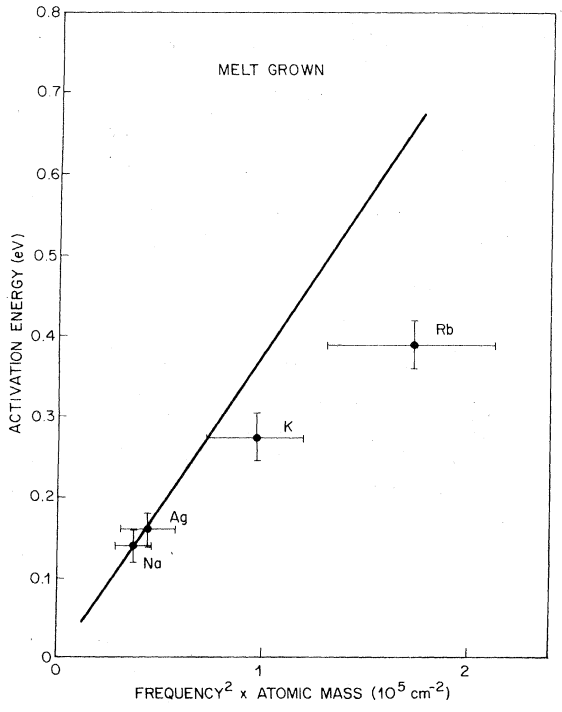

FIG. 14. Activation energy vs square of the-low frequency edge of the infrared-absorption band. Melt grown. Solid line is Eq. (6).

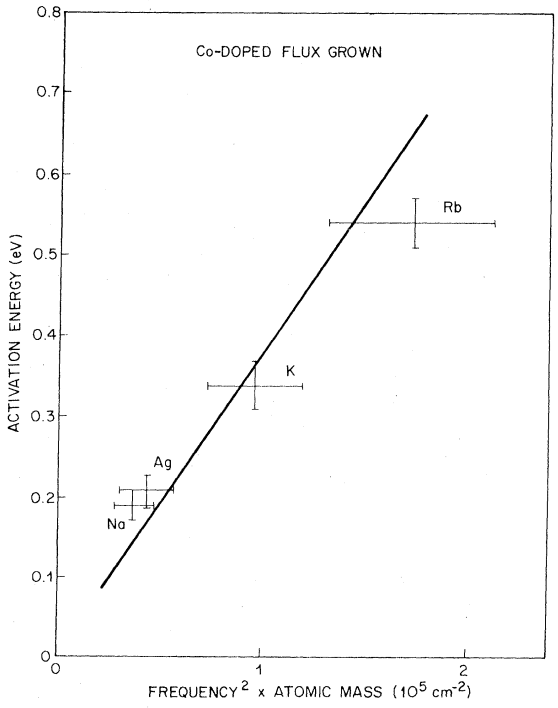

FIG. 15. Activation energy vs square of the-low-frequency edge of the infrared absorption band. Co-doped flux grown. Solid line is Eq. (6).

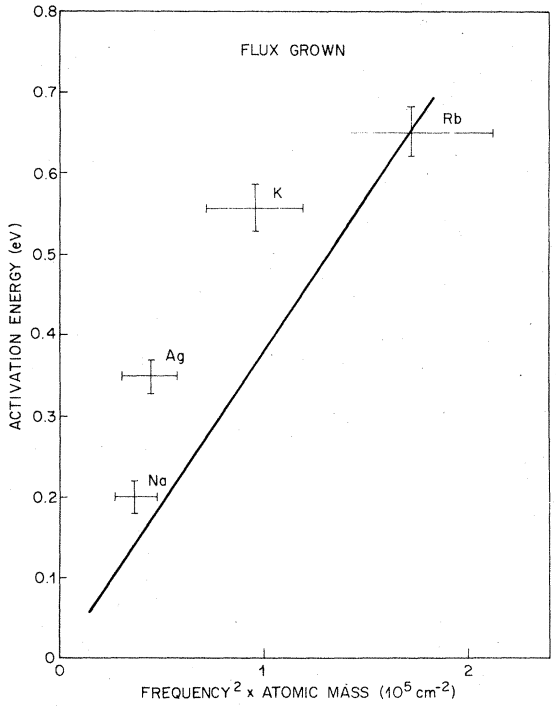

FIG. 16. Activation energy vs square of the low-frequency edge of the infrared absorption band. Flux grown. Solid line is Eq. (6).

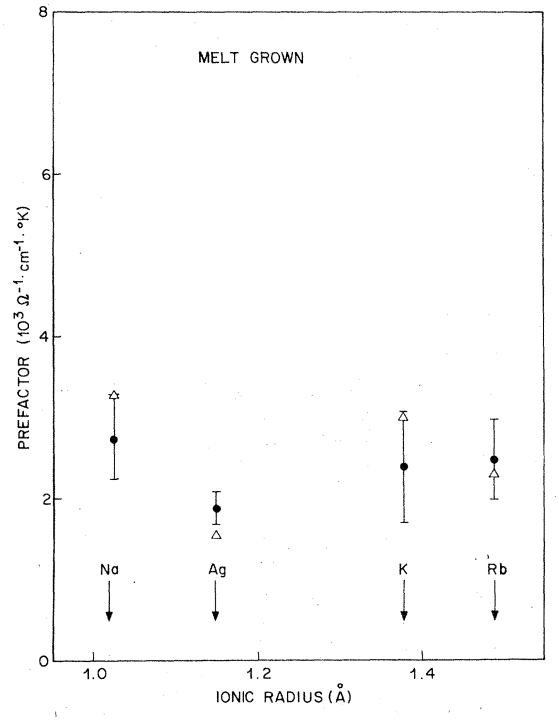

FIG. 17. Prefactors vs ionic radius. Δ—Predictions of Wang, Gaffari and Choi. Melt grown.

infrared bands for each cation. Following WGC, we assume that the interstitial pair move in a sinusoidal potential to the saddle point. Then we expect

$$E_a = \tfrac{4}{3} f_0^2 M a^2 , \tag{6}$$

where f_0 is the frequency of the pair in the direction of the saddle point, assumed near the low-frequency edge of the infrared absorption, M is the atomic mass, and a is the unit-cell dimension in the diffusion plane. Although we have difficulty accepting WGC's value for the Ag activation energy, we can include it in Figs. 14–16, if we use the experimental vibration frequencies. Presumably the interstitialcy mechanism is still operative in Ag β-alumina but one reverses the role of the saddle point and local minima obtained for the alkalis (see Fig. 3).

The solid line is the prediction of (6). We can see that good agreement is achieved for the melt- and Co-doped flux-grown material while less satisfaction is found with the pure flux-grown material. At first glance, there is striking and convincing correlation between the activation energies and vibrational frequencies.

We make the same comparison for the observed prefactors and those predicted by WGC. Following WGC, we scale the prefactors by $(n/N)[(1-n)/N]$ where n/N is the excess mobile cation. In Figs. 17–19, we again see good agreement for the melt and Co flux grown, but poor agreement for the pure flux grown. In fact, qualitative agreement is lost for the pure flux-grown material where Ag, which should have the smallest prefactor, is observed to have the largest. If we restrict our attention to the material with the highest conductivity, the melt and Co-doped flux, we see again remarkably good quantitative agreement with a rather naive view of diffusion in this system.

At this point, we would like to digress and discuss the prefactor and its relation to vibration frequencies observed near equilibrium. We make reference to an early paper by Vineyard.[45] Using absolute rate theory, Vineyard has shown that the attempt frequency is given by

$$\nu^* = \left(\prod_{j=1}^{N} \nu_j \right) \Big/ \left(\prod_{j=1}^{N-1} \nu_j' \right) , \tag{7}$$

where ν_j' are the $N-1$ normal modes when the system is at the saddle point, the mode with imaginary frequency that carries the system to its new equilibrium being excluded. At worst, for a strongly interacting system where there are no well-defined localized modes for the diffusing species, it seems clear that the effective attempt

frequency ν^* will not be simply related to any single equilibrium vibrational frequency. At best, for vacancy diffusion with all the diffusing species vibrating as Einstein oscillators in a rigid host lattice, the attempt frequency will be the equilibrium vibration of the diffusing species.

The indirect interstitial or interstitialcy mechanism is sufficiently complex that even in the simplest of all possible situations, where the host is perfectly rigid, expression (7) will not lead simply to the vibrations of the interstitial pair at equilibrium. This is due to the fact that the interstitialcy mechanism involves by its very nature interactions between diffusing species, and the normal modes at the saddle point will not be simply related to the normal modes at equilibrium. Nevertheless, if the diffusion can be considered to take place in a rigid host lattice, the normal modes that do not cancel out of expression (7) will involve only mobile cation motion, and it is probably not surprising that the equilibrium vibrational frequencies observed by infrared absorption and the attempt frequency used for the observed prefactor should at least scale appropriately and differ from one another by factors close to unity.

These difficulties are not relevant to the relation between the activation energy and the equilibrium vibrations of the defect (6). That may be criticized only for invoking a sinusoidal potential as suitable approximation to the energy barrier.

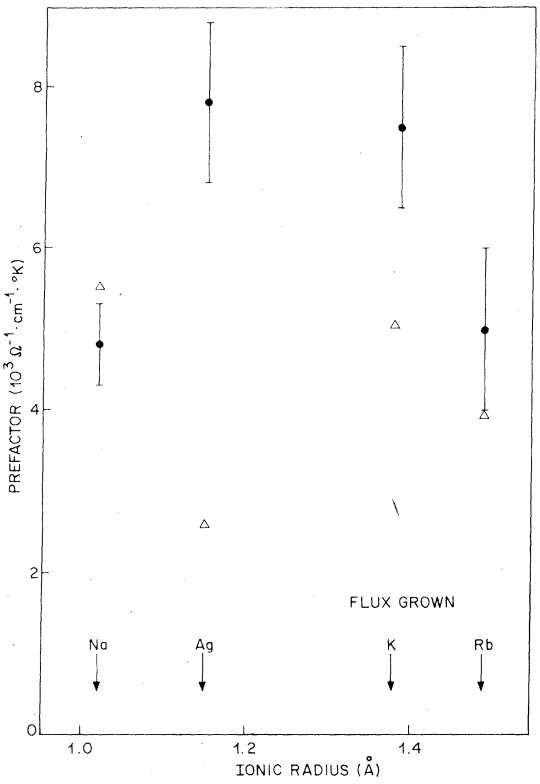

FIG. 19. Prefactors vs ionic radius. Δ—Predictions of Wang, Gaffari, and Choi. Flux grown.

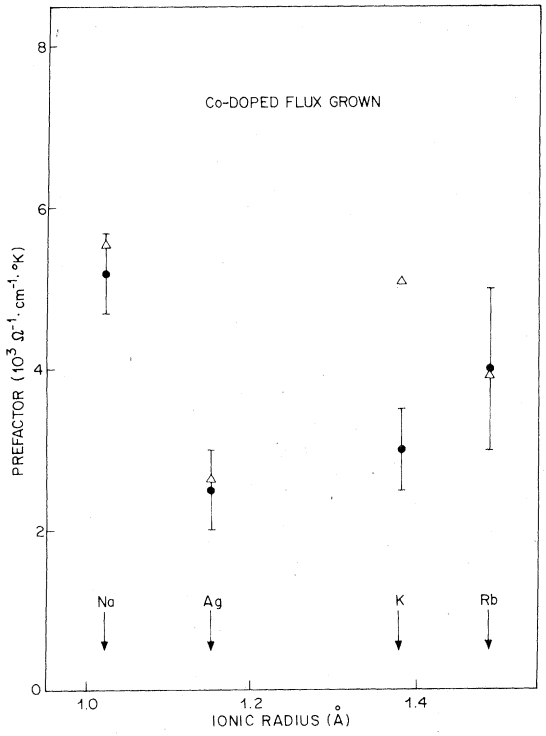

FIG. 18. Prefactors vs ionic radius. Δ—Predictions of Wang, Gaffari, and Choi. Co-doped flux grown.

There seems to be a more basic difficulty in our understanding of the attempt frequency that has been brought to light by the nuclear spin-lattice relaxation measurements of Walstedt *et al.*[27] and subsequently by the internal friction measurements of Barmatz *et al.*[35] The NMR experiments invariably give attempt frequencies an order of magnitude smaller than those obtained either from the far infrared or dc conductivity. The internal friction measurements tend to support the NMR result but it should be made clear that if activation energies consistent with the conductivity data are used in the analysis of the internal friction measurements, attempt frequencies consistent with the far infrared will result.

Recent theory by Brawer[46] on potential barrier hopping appears to bear on this point. He argues that harmonic oscillation about a local minimum is Markovian only on a time scale that is substantially longer than the inverse of the vibrational frequency and hence one might expect attempt frequencies substantially smaller than the actual

vibrational frequencies. If forced to abandon the vibrational frequencies as a measure of attempt frequency, we are still left with the attempt frequency determined from diffusion coefficient, and ionic conductivity which remains an order of magnitude larger than the NMR determined attempt frequency. At present the discrepancy between the attempt frequency determined by NMR, internal friction, conductivity, diffusion, and infrared vibrations remains a glaring defect in our understanding.

V. CONCLUSIONS

At first glance, it appears from the correlation between the vibrational properties and dc conductivity that the basic entity or mechanism is the interstitialcy jump first proposed by Whittingham and Huggins[14,21] and that the interactions that control the barrier heights and attempt frequencies are properly parameterized by the model calculation of Wang, Gaffari, and Choi. The picture that emerges is one in which the ions move in a rigid host lattice which provides a potential energy surface for the collection of mobile ions to move. The most important mobile-ion–mobile-ion interaction is that leading to the interstitial pair and its subsequent motion over the barrier. The interaction with other mobile ions is important in that relaxation of the neighboring mobile ions around their equilibrium positions does lead to a reduction in vibrational frequencies and barrier heights.

However, it is also clear that agreement with this simple model is not perfect and that the prefactor and activation energy can be altered by growth conditions and chemical content. These changes are not so large as to suggest that the basic mechanism of diffusion has been altered, but do lead to substantial and important changes in the observed conductivity primarily through the exponential dependence on activation energy. These changes are probably related to the large concentration of interstitial pairs that inevitably interact with each other and the defects that compensate the extra mobile cations. It has been demonstrated that the degree of short-range order depends on mobile-ion and growth conditions. Presumably, the kind of compensation will also play an important role. It appears that a full understanding of this complex system will be had only after we appreciate in a quantitative manner the role short-range order and compensation play in inhibiting diffusion in this system.

ACKNOWLEDGMENTS

We would like to acknowledge the many useful discussions with our colleagues D. B. McWhan, P. D. Dernier, R. E. Walstedt, M. Barmatz, with Professor Sang-il Choi at the University of North Carolina, and with Professor L. L. Chase at the University of Indiana.

[1]See J. R. Birk, in *Superionic Conductors*, edited by G. D. Mahan and W. L. Roth (Plenum, New York, 1976), p. 1.
[2]J. D. Busi and L. R. Turner, J. Electrochem. Soc. 121, 183C (1974).
[3]N. Weber, Energy Convers. 14, 1 (1974).
[4]N. Weber, in Ref. 1, p. 37.
[5]J. T. Kummer and N. Weber, Trans. Soc. Adv. Electrochem. Sci. Technol. 76, 1003 (1968).
[6]J. L. Sudworth and M. D. Hames, in *Power Sources*, edited by D. H. Collins (Oriel, Stocksfield, England, 1970), Vol. 3, p. 227.
[7]L. J. Miles and I. Wynn Jones, in Ref. 6, p. 245.
[8]C. A. Beevers and M. A. S. Ross, Z. Kristallogr. Kristallgeom. Kristallphys. 97, 59 (1937).
[9]C. R. Peters, M. Bettman, J. W. Moore, and M. D. Glick, Acta Crystallogr. B 27, 1826 (1971).
[10]W. L. Roth, J. Solid State Chem. 4, 60 (1972).
[11]J. T. Kummer, Prog. Solid State Chem. 7, 141 (1972).
[12]W. L. Roth, F. Reidinger, and S. LaPlaca, in Ref. 1, p. 223.
[13]H. Sato and Y. Hirotsu, Mater. Res. Bull. 11, 1307 (1976).
[14]M. S. Whittingham and R. A. Huggins, J. Electrochem. Soc. 118, 1 (1971).
[15]W. L. Roth, Trans. Am. Crystallogr. Assoc. 11, 51 (1975).
[16]D. B. McWhan, P. D. Dernier, C. Vettier, and J. P. Remeika, in Ref. 1, p. 376; and (unpublished).
[17]F. Reidinger, Ph.D. thesis (State University of New York, Albany, 1977) (unpublished).
[18]D. B. McWhan, S. J. Allen, Jr., J. P. Remeika, and P. D. Dernier, Phys. Rev. Lett. 35, 953 (1975); 36, 344(E) (1976).
[19]Y. LeCars, R. Comès, L. Deschamps, and J. Thiery, Acta Crystallogr. A 30, 305 (1974).
[20]J. P. Boilot, G. Collin, R. Comès, J. Thiery, R. Collongues, and A. Guinier, in Ref. 1, p. 243.
[21]M. S. Whittingham and R. A. Huggins, J. Chem. Phys. 54, 414 (1971).
[22]D. B. McWhan, S. M. Shapiro, J. P. Remeika, and G. Shirane, J. Phys. C 8, L487 (1975).
[23]S. M. Shapiro, in Ref. 1, p. 261.
[24]H. S. Story, W. C. Bailey, I. Chung, and W. L. Roth, in Ref. 1, p. 317, and references therein.
[25]D. Jerome and J. P. Boilot, J. Phys. (Paris) 35, L129 (1974).
[26]J. P. Boilot, L. Zuppipoli, G. Delplanque, and D. Jerome, Philos. Mag. 32, 343 (1975).
[27]R. E. Walstedt, R. Dupree, J. P. Remeika, and

A. Rodriguez, Phys. Rev. B 15, 3442 (1977).
[28]D. B. McWhan, J. P. Remeika, F. L. S. Hsu, and C. M. Varma, Phys. Rev. B 15, 553 (1977).
[29]P. J. Anthony and A. C. Anderson, Phys. Rev. B 14, 5198 (1976).
[30]C. H. Hao, L. L. Chase, and G. D. Mahan, Phys. Rev. B 13, 4306 (1976).
[31]L. L. Chase, C. H. Hao, and G. D. Mahan, Solid State Commun. 18, 401 (1976).
[32]U. Strom, P. C. Taylor, S. G. Bishop, T. L. Reinecke, and K. L. Ngai, Phys. Rev. B 13, 3329 (1976).
[33]A. S. Barker, Jr., J. A. Ditzenberger, and J. P. Remeika, Phys. Rev. B 14, 4254 (1976).
[34]A. S. Barker, Jr., J. A. Ditzenberger, and J. P. Remeika, Phys. Rev. B 14, 386 (1976).
[35]M. Barmatz and R. Farrow, 1976 Ultrasonics Symposium Proceedings, IEEE Cat. No. 76, CH1120-5SU, p. 662 (unpublished).
[36]R. D. Armstrong, P. M. A. Sherwood, and R. A. Wiggins, Spectrochim. Acta A 30, 1213 (1974).
[37]S. J. Allen, Jr. and J. P. Remeika, Phys. Rev. Lett. 33, 1478 (1974).
[38]S. J. Allen, Jr., L. C. Feldman, D. B. McWhan, J. P. Remeika, and R. E. Walstedt, in Ref. 1, p. 279.
[39]H. Sato and R. Kikuchi, J. Chem. Phys. 55, 677 (1971); R. Kikuchi and H. Sato, *ibid.* 55, 702 (1971).
[40]J. C. Wang, M. Gaffari, and Sang-il Choi, J. Chem. Phys. 63, 772 (1975).
[41]P. D. Dernier and J. P. Remeika, J. Solid State Chem. 17, 245 (1976).
[42]W. Y. Hsu, Phys. Rev. B 14, 5161 (1976).
[43]P. B. Klein, D. E. Schafer, and U. Strom, Bull. Am. Phys. Soc. 22, 370 (1977).
[44]J. H. Kennedy and A. F. Sammells, J. Electrochem. Soc. 119, 1609 (1972).
[45]G. H. Vineyard, J. Phys. Chem. Solids 3, 121 (1957).
[46]S. Brawer, Phys. Rev. B 10, 3287 (1974).